

Silvernano Particle Loaded on Activated Carbon as Novel Adsorbent for the Removal of Acid Yellow 199 Dye

Z. Alishavandi¹, N. Mosallanejad^{*2}, R. shabani³

¹Graduate student, Department of Chemistry, Firozabad Branch, Islamic Azad University, Firozabad, Iran

²Department of Chemistry, Mashhad Branch, PN University, Khorasan, Iran

³Department of Chemistry, Firozabad Branch, Islamic Azad University, Firozabad, Iran

(Received: 15 July 2013

Accepted: 10 August 2013)

Abstract: In this study, a new adsorbent, silver nanoparticle loaded on activated carbon (Ag-NP-AC) was used for removal of acid yellow 199 (AY 199) dye. This novel material was characterized and identified by different techniques such as Brunauer, Emmett and Teller (BET), field emission scanning electron microscopy (FESEM), X-ray diffraction (XRD) analysis. Unique properties of this adsorbent such as high surface area ($>1100 \text{ m}^2\text{g}^{-1}$) and low pore size ($<47 \text{ \AA}$) and average particle size lower than 60 \AA make it possible for efficient removal of Ay199. In batch experimental set-up, adsorbent dosage, initial dye concentration, contact time and pH were investigated. Optimum values were set as pH of 3.0, 0.03g/50mL of adsorbent for initial dye concentration of 15 mgL^{-1} at 40 min and $25 \pm 1 \text{ }^\circ\text{C}$. The adsorption of Ay199 follows the pseudo-second-order rate equation in addition to interparticle diffusion model (with removal more than 90%) at all conditions. Equilibrium data fitted well with the Langmuir model, while maximum adsorption capacity was 30 mg g^{-1} for 0.03 g/50mL of Ag-NP-AC. Calculation of various thermodynamic parameters such as, Gibb's free energy, entropy and enthalpy of the on-going adsorption process also indicated feasibility and endothermic nature of AY 199 adsorption onto Ag-NP-AC.

Keywords: Adsorption, Acid yellow 199, Silver nanoparticle loaded on activated carbon, Kinetic, equilibrium and thermodynamic,

INTRODUCTION

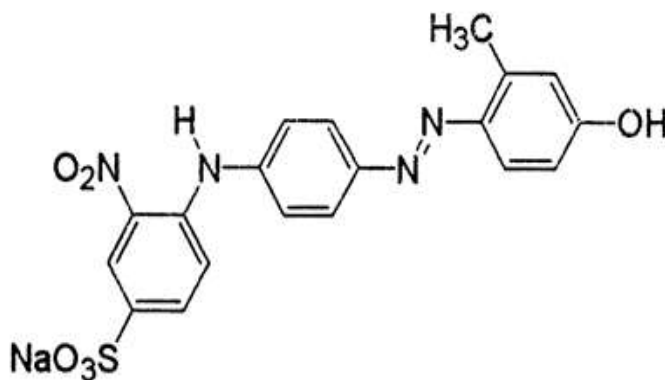
Water bodies consisting of both polluted wastewaters and groundwater from the seas, rivers and lakes are of special concern to people working in water purification and the environment in general. Organic dyes came up as one of the many new chemicals which could be used in many industrial activities. One of these dyes is Acid Yellow 199 (Scheme.1.) that due to the extensive use of this dye in industries, it has become an integral part of industrial effluent [1]. This dye is toxic and potentially carcinogenic in nature and its

removal from the industrial effluents is a major environmental problem [2-6]. In humans AY 199 causes irritation to the gastrointestinal tract; symptoms include nausea, vomiting and diarrhea. It also causes irritation to the respiratory tract, leads to cough and shortness of breath. Skin contact causes irritation with redness and pain. Conventional wastewater treatment protocol based on physicochemical, chemical and biological process is divided into different branches including coagulation and flocculation [7], adsorption [8], Biosorption[9], electrochemical

Corresponding Author: Narges Mosallanejad, Department of chemistry, Mashhad Branch, PN University, Khorasan, Iran, Email: nargesmosallanejad@yahoo.com

techniques [10] and fungal decolonization [11]. Among these procedures, adsorption is applicable for large-scale biochemical and purification applications [12]. This technique benefits from unique properties such as simple design, using nontoxic and low cost adsorbents and high efficiency. Characteristics and appropriate selection of adsorbent are based on remarks such as removal capacity, treatment cost and operating conditions [13]. Nano scale material benefit from advantages such as high surface reactive atom, large surface area with porous structure. These advantages improve the adsorption efficiency for

dye removal. Silvernano particles due to their ordered structure, high aspect ratio, ultra-light weight, high mechanical strength and high surface area are suitable for adsorption [14-17]. This study reports on the feasibility of applying Ag-NP-AC as low-cost adsorbent for AY 199 removal from aqueous solution. The effects of adsorbent dosage, initial AY 199 concentration and pH were studied on AY 199 adsorption onto Ag-NP-AC. Thermodynamic and adsorption kinetics and isotherms parameters were also evaluated and reported.



Scheme 1. Chemical structure of Acid yellow 199

EXPERIMENTAL

Materials

The Acid yellow 199 (AY 199) dye [CAS = 70865-20-2, chemical formula = C₁₉H₁₅N₄NaO₆S, FW = 450.405; nature = basic yellow] was supplied by Sigma-Aldrich (M) SdnBhd, Malaysia and used as received. Applied reagents such as NaOH, HCl and KCl with the analytical reagent grade were purchased from Merck (Darmstadt, Germany). Stock AY 199 solution was prepared by dissolving its appropriate amount in double distilled water and the test solutions were prepared by diluting stock solution to the desired concentrations, while its concentration was determined at 386.4 nm.

Instrumentation

The pH measurements were done using pH/Ion meter model-686, and absorption measurements were carried out using Jusco UV-Visible spectrophotometer model V-570 using a quartz cell with an optical path of 1 cm. The morphology and size distribution of the Ag nanoparticles were determined by a Hitachi H-800 TEM at an operating voltage of 200 Kv. The X-ray diffraction patterns (XRD) were recorded on a Bruker D₈ advance X-ray diffractometer using the CuK α ($\lambda=1.5406$ Å) radiation, with a scanning speed of 1° per min, 35 kV and 30 mA and 2θ scan over 2 to 70°. A BET surface analyzer (Quantachrome NOVA 2000, USA) was used to measure nitrogen adsorption-desorption isotherm at 77 K. Before each study, the samples were degassed via helium

purging at 553 K for 3 h. The BET experiments give useful information on the adsorbent properties such as surface area, total pore volume and micro pore area.

Preparation of Ag-NP-AC

The Ag nanoparticles were synthesized in a one-step reduction process in an aqueous solution [18]. All reactions were carried out in oxygen free water under nitrogen. In a typical preparation, a 400 μ L aliquot of a 0.1 M AgNO₃ aqueous solution was added into 100 mL of an aqueous solution containing 0.15 wt % of the soluble starch and vigorously stirred for 1 h. The pH of resulting solution was adjusted to 8.0 by adding a 0.1 M NaOH solution. Under this experimental condition, the initial reaction mixture was colorless and the growth of the Ag nanoparticles was monitored at different intervals using UV-visible absorption spectroscopy. After about 1 h the solution turned light yellow, which indicated the initial formation of the Ag nanoparticles. The mixture was maintained at 50 °C for 24 h and the color of the reaction solution became yellow. The Ag nanoparticles were loaded in a high surface activated carbon produced from coconut husk, a popular agricultural waste in Vietnam by thermal activation. The surface area of the best activated carbon is 890 m²/g. The presence of Ag nanoparticles does not change significantly properties of the activated carbon in terms of morphology.

Measurements of dye uptake

The concentrations of dye in solution were estimated quantitatively using the linear regression equations obtained by plotting its calibration curve over AY199 concentrations. The efficiency of AY 199 removal was determined at certain time intervals in the range of 0–40 min and the equilibrium was established after 20 min. The effect of pH on AY 199 adsorption was studied by adjusting pH of dye solutions (15 mg L⁻¹) in the

pH range of 1–8 using 0.03 g/50mL of Ag-NP-AC for 40 min, while the initial pH of solution was adjusted by addition of HCl or NaOH. Dye adsorption experiments were also accomplished to obtain isotherms in the range of 10–40mg L⁻¹ AY 199 concentrations with 300 rpm in an isothermal shaker at room temperature. The concentration of the AY 199 in the solution after equilibrium adsorption was measured by a double beam UV-vis spectrophotometer at 386.4 nm. The amount of adsorbed AY199 at equilibrium (q_e (mg/g)) was calculated by:

$$q_e = (C_0 - C_e) V/W \quad (1)$$

Where C_0 and C_e (mgL⁻¹) are the liquid-phase concentrations of dye at initial and equilibrium, respectively. V (L) is the volume of the solution and W (g) is the mass of dry adsorbent used.

RESULTS AND DISCUSSION

Characterization of Ag-NP-AC

Figure 1 shows the UV-Vis absorption spectra obtained at different time intervals after mixing AgNO₃ aqueous solution with soluble starch aqueous solution at 50 °C. Formation of Ag nanoparticles in the colloidal solution was monitored from their absorption spectra as the small noble metal particles reveal absorption band in the UV-Vis spectral region due to surface Plasmon resonance (SPR) [19]. The process of reduction of the Ag⁺ ions using the starch was slow, yielding a broad absorption band centered at about 400 nm until 1 h of reaction, which was assigned to the SPR of Ag nanoparticles. The broadband indicates relatively high poly dispersity, both in size and shape of the Ag particles. The intensity of the SPR band increased systematically with the increase of reaction time, to reach a maximum after about 24 h. Thereafter, the intensity of the SPR band did not change. The reduction of Ag⁺ ions with starch aqueous solution at 50 °C leads to the formation of Ag nanoparticles

that are stable in solution for several months. This indicates that the soluble starch serves as both reducing and protecting agent. X-ray diffraction (XRD) pattern of silver nanoparticles powder is shown in Figure 2. The pattern exhibits peaks at 2θ angles of 38.17, 44.21, 64.32, and 77.12 that correspond to the [111], [200], [220], and [311] crystal planes of a cubic lattice structure of silver nanoparticles, respectively [20]. From the full-width at half-maximum of diffraction peaks, the average size of the silver nanoparticles has been calculated using the Debye-Scherrer equation [21]. The calculated average size of Ag nanoparticles was around 55 nm. The field emission scanning electron microscopy FESEM image of the Ag nanoparticles is shown in Figure 3 which reveals that the Ag nanoparticles are semi-spherical in shape and quite uniform in size distribution. The size of each Ag nanoparticles is in the range of

15–80 nm. The particle size measured directly from this FESEM image agrees with that determined by the XRD results. Determination of specific surface area by $N_2/77$ K adsorption isotherms assumed to measure the surface area in microspores within pore sizes of a material [18]. Specific surface area (SSA) is the accessible area of adsorbent surface per unit mass of material. The interference by the surrounding phase is especially problematic for the Bruner-Emmet-Teller (BET) N_2 adsorption/desorption isotherm method because the entire surface is modified by vacuum treatment before N_2 adsorption. Table 1 and Figures 4-8 show that adsorbent possessed appreciable narrow micro-porosity. The surface area of Ag-NP-AC was found to be $1174.57\text{m}^2\text{g}^{-1}$. Total pore volume is $0.6\text{cm}^3\text{g}^{-1}$. Total surface properties of adsorbent are presented in Table 1.

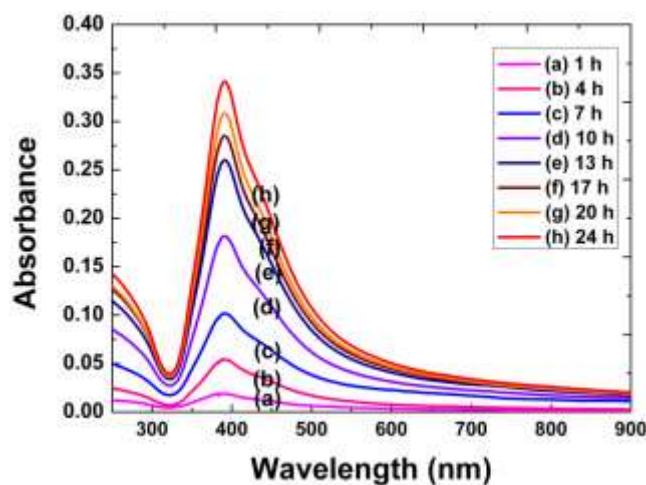


Figure 1. Temporal evolution of UV-visible absorption spectra after addition of AgNO_3 solution into soluble starch solution at 50°C .

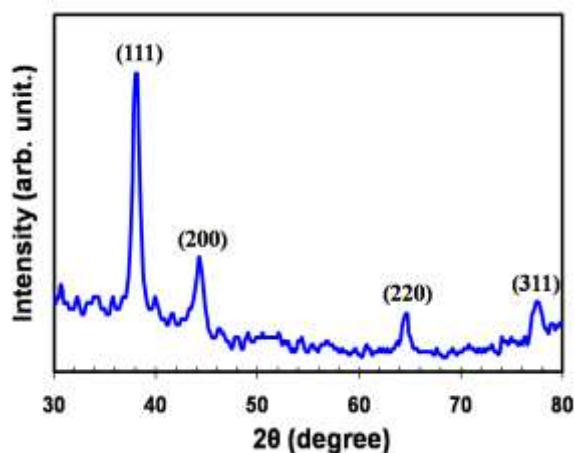


Figure 2. X-ray diffraction pattern of the starch-stabilized Ag nanoparticles.

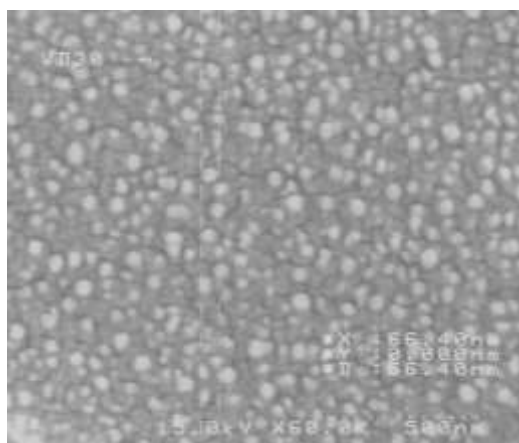


Figure 3. FESEM image of the Ag nanoparticles loaded onto activated carbon.

Table 1 Summary Report of adsorbent properties

Summary Report	
Surface Area	
BET Surface Area:	1174.5738 m ² /g
BJH Adsorption cumulative surface area of pores between 17.000 Å and 3000.000 Å width:	97.472 m ² /g
BJH Desorption cumulative surface area of pores between 17.000 Å and 3000.000 Å width:	99.0939 m ² /g
Pore Volume	
BJH Adsorption cumulative volume of pores between 17.000 Å and 3000.000 Å width:	0.097163 cm ³ /g
BJH Desorption cumulative volume of pores between 17.000 Å and 3000.000 Å width:	0.096101 cm ³ /g
Pore Size	
Adsorption average pore width (4V/A by BET):	29.4940 Å
BJH Adsorption average pore width (4V/A):	46.163 Å
BJH Desorption average pore width (4V/A):	42.278 Å
Nanoparticle Size	
Average Particle Size :	57.075 Å

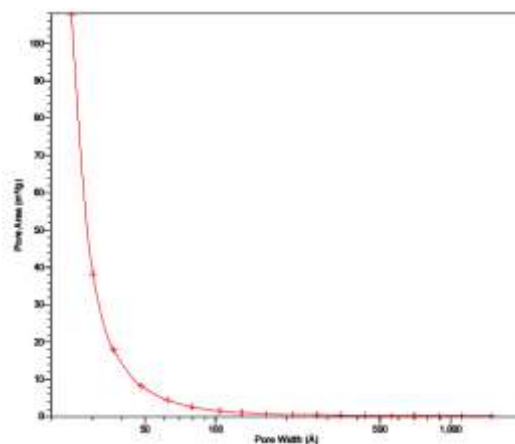


Figure 4. BJH Adsorption Cumulative Pore Volume (Larger) Halsey :Faas Correction

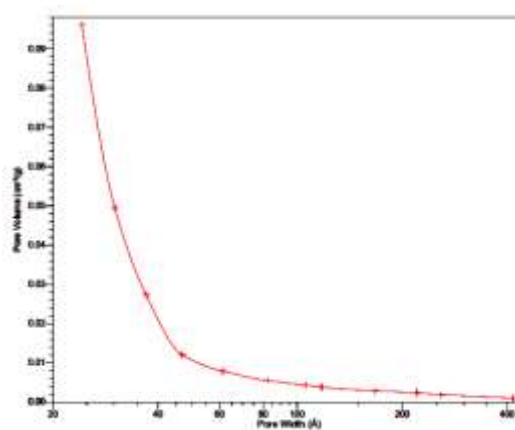


Figure 5. BJH Desorption Cumulative Pore Area (Larger) Halsey :Faas Correction

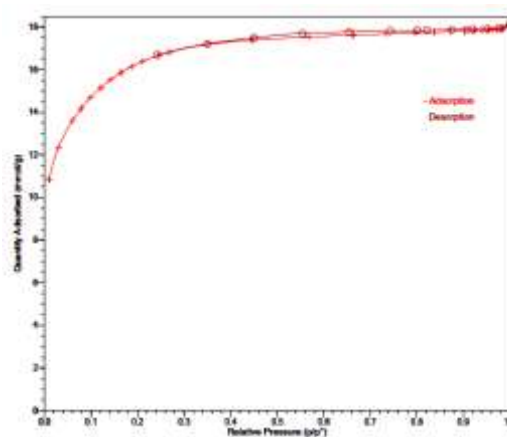


Figure 6. Isotherm Linear Plot

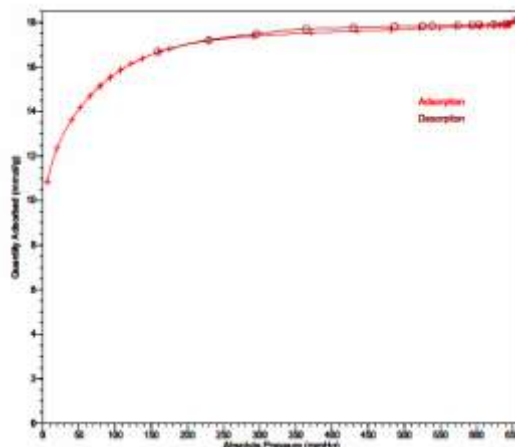


Figure 7. Isotherm Linear Absolute Plot

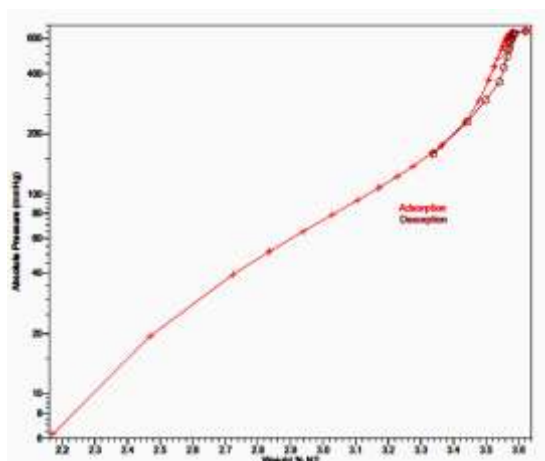


Figure 8. Isotherm Pressure Composition

Effect of system pH on AY199 Uptake

The wastewater from textile industries usually has a wide range of pH values. Thus pH of the system plays an important role in the textile wastes treatment. The value of pH affects both aqueous chemistry and surface binding sites of the adsorbents. The effect of initial pH on the adsorption of AY 199 was studied in the pH range

of 1 to 8 at room temperature at initial dye concentration of 15 mgL^{-1} , adsorbent dose of 0.03 g/50 mL and contact time of 30 min and respective results are presented in (Figure 9). As it can be seen, the maximum uptake of the AY 199 is obtained at pH of 3.0. It was observed, that the pH significantly affects the extent of adsorption of dye over the adsorbent and a decrease was observed in

the adsorption efficiency further this value. At lower pH, probably surface of Ag- NP-AC has positive charge (protonation of functional group of

Ag-NP-AC in highly acidic solution) which favors the adsorption of AY 199 over Ag-NP-AC and leads to increase in adsorption.

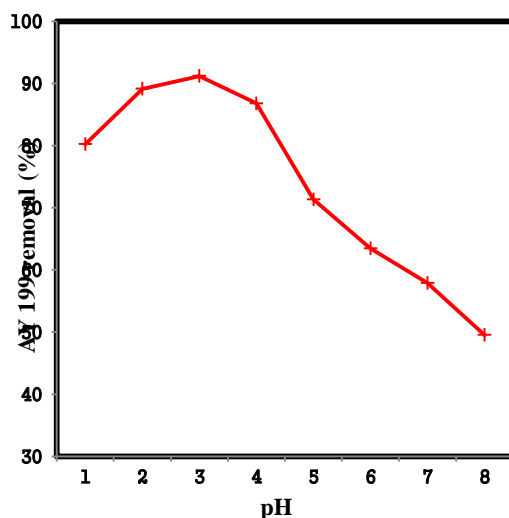


Figure 9. Effect of system pH on adsorption of AY 199 (15mg L^{-1}) onto Ag-NP-AC (0.03g) at room temperature ($25\pm 1\text{ }^\circ\text{C}$), agitation speed 300 rpm for the maximum contact time required to reach the equilibrium (40 min).

Effect of contact time

Equilibrium time is one of the most important parameters in the design of economical wastewater treatment system. The adsorption of dyes onto Ag-NP-AC was studied as a function of contact time in order to determine the necessary adsorption equilibrium time. Rapid uptake and quick establishment of equilibrium time implies the efficiency of particular adsorbent in terms of usage in wastewater treatment. Figure 10 shows the effects of contact time on adsorption of dye by Ag-NP-AC and It was found that more than 50% of AY 199 removal occurs in the first 2 min. Subsequently, the adsorption rate changes slightly due to decrease in diffusion rate and concentration

gradient. Later slow rate of AY 199 adsorption is probably due to the electrostatic repulsion between the positive charges adsorbed molecules and respective ones in the bulk in coincide to the slow pore diffusion of the solute ions into the bulk of the adsorbent. It can be seen that the final equilibrium time significantly depends on the initial dye concentration and amount of adsorbent. At each initial dye concentration, the increases in adsorbent mass enhance the AY 199 diffusion and subsequently decrease the time for complete dye removal. The equilibrium removal time at 15 mgL^{-1} for adsorbent mass of 0.03g/50mL was in 20 min and the removal percentage was 95%.

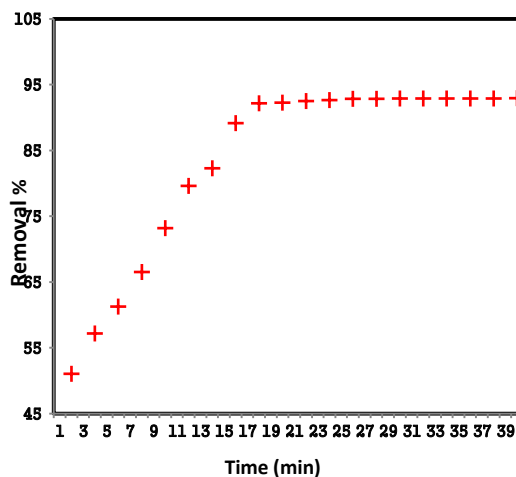


Figure10. Effect of contact time on the removal of different adsorbent of Ag-NP-AC in concentration 15 mg L^{-1} of AY 199 at pH 3.0.

Effect of initial dye concentration on adsorption of AY 199

The influence of dye concentration on the adsorption of the dye is shown in Figure 11. When the dye concentration increases from $10\text{-}40 \text{ mgL}^{-1}$, the percentage of dye adsorbed decreases from 90.1% to 32%. The result shows that the % removal depends on the initial dye concentration. In case of low dye concentrations, the ratio of the

initial number of moles of the dye ions to the available surface area of adsorbent is large and subsequently the fractional adsorption becomes independent of initial concentration. However, at higher dye concentrations, the available sites of adsorption are fewer, and hence the percentage removal of metal ions which depends upon the initial concentration, decreases.

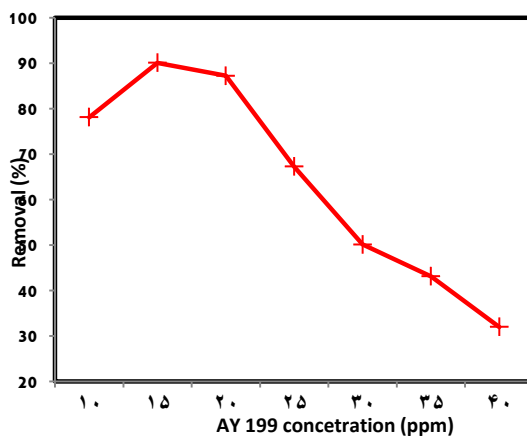


Figure 11. Effect of initial dye concentration on the adsorption of AY 199

Effect of adsorbent dosage

One of the most critical parameter for rapid and efficient dye removal is size and amount of adsorbent which must be optimized. The adsorbent dose is an important parameter in adsorption studies because it determines the capacity of adsorbent for a given initial concentration of dye solution. The effect of adsorbent dose on the dye removal percentage was shown in Figure 12. It was observed that initially the removal percentage

increased rapidly with the increase in adsorbent dose till 0.035 g and after the critical dose the removal percentage almost reached a constant value. This can be attributed to increase adsorbent surface area and availability of more adsorption sites with the increasing dosage of the adsorbent, while the adsorption density of dye decreased with increasing in adsorbent dosage. Therefore, for subsequent work 0.03 g of Ag-NP-AC has been selected.

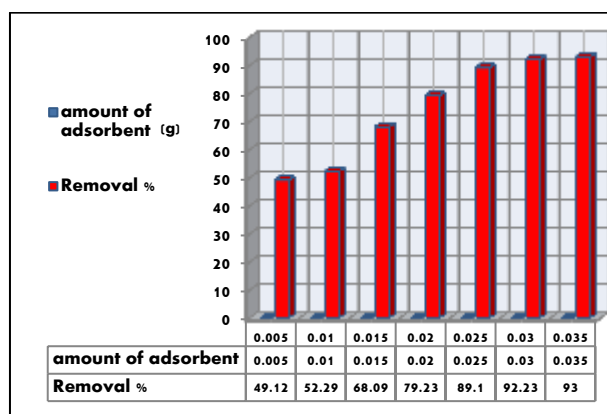


Figure 12. Effect of adsorbent dosage on AY 199 removals in the range of .005-0.035 g at (pH 3.0, agitation speed: 300 rpm, temperature: 25±1 °C).

Effect of temperature

In order to observe the effect of temperature on the adsorption capacity, experiments were carried out for the dye concentration of 15 mg L⁻¹ and at different temperatures in the range of

283.15-333.15 K using 0.03 g of adsorbent. Figure 13. shows that increasing temperature, leads to improve in adsorption capacity that it can be explained by the endothermic spontaneity of the adsorption process.

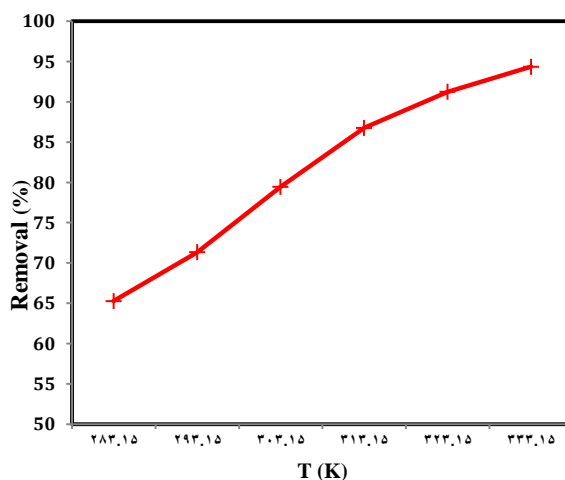


Figure 13. Effect of temperature on removal of AY 199 at 0.03g of Ag-NP-AC, pH 3, dye concentration of 15 mg L⁻¹

Equilibrium isotherms

Adsorption equilibrium isotherm represents mathematical relation of amount of adsorbed target per gram of adsorbent (q_e (mg g^{-1})) to the equilibrium solution concentration (C_e (mgL^{-1})) at fixed temperature. This investigation has great attention from both theoretical and practical point of view to obtain strong knowledge about surface properties of adsorbent and removal mechanism [22].

Langmuir isotherm

The Langmuir isotherm is based on the assumption that the adsorption process takes place at specific homogeneous sites within the adsorbent surface and that once a dye molecule occupies a site, no further adsorption can take place at that site, which concluded that the adsorption process is monolayer in nature. The Langmuir equation, which is valid for monolayer adsorption onto a completely homogenous surface with a finite number of identical sites with negligible

interaction between adsorbed molecules, is represented in the linear form as follows [23]:

$$C_e/q_e = 1/k_L Q_m + C_e/Q_m \quad (1)$$

where K_L is the Langmuir adsorption constant (L mg^{-1}) and Q_m is the theoretical maximum adsorption capacity (mg g^{-1}). The value of Q_m and K_L constant is obtained by The Langmuir plot (C_e/q_e vs. C_e) that these values and the correlation coefficient of this model is presented in Table 2. The isotherm of AY 199 on Ag-NP-AC was found to be linear over the whole concentration range studied and the correlation coefficient was extremely high ($R^2 > 0.99$) as shown in Table 2.

Table 2 isotherm constants of AY 199 adsorption onto Ag-NP-AC

Isotherm	Equation	Parameters	Value
Langmuir	$C_e/q_e = 1/K_a Q_m + C_e/Q_m$	Q_m (mg g^{-1})	30
		K_a (L mg^{-1})	0.275
		R_L	0.26
		R^2	0.9916
		X^2	0.0763
Freundlich	$\ln q_e = \ln K_F + (1/n)\ln C_e$	R^2	0.9595
		$1/n$	0.589
		K_F (L mg^{-1})	2.23
		X^2	0.206
Tempkin	$q_e = B_1 \ln K_T + B_1 \ln C_e$	R^2	0.989
		B_1	6.49
		K_T (L mg^{-1})	2.69
		X^2	0.0934

Freundlich isotherm

The Freundlich isotherm is derived by assuming a heterogeneous surface with a non-uniform distribution of sorption heat over the surface was presented in the linear form as follows [24]:

$$\text{Log}q_e = \text{log}K_F + 1/n_F \text{log}C_e \quad (2)$$

K_F shows information about the bonding energy and is known as the adsorption or distribution coefficient and represents the quantity of dye adsorbed onto adsorbent. $1/n$ shows adsorption intensity of dye onto the adsorbent (surface heterogeneity). The value becomes closer to zero by rising heterogeneous nature of surface ($1/n < 1$ indicates normal Langmuir isotherm while $1/n$ above 1 indicate bi-mechanism and cooperative adsorption). The applicability of the Freundlich adsorption isotherm was assessed by plotting $\log(q_e)$ versus $\log(C_e)$ and respective values for this model constant at various amount of adsorbent is shown in Table 2. The correlation coefficient (0.959) and higher error value of this model shows that the Freundlich model has lower efficiency compare to the Langmuir model.

Tempkin isotherm

Judgment for suitability of each model for the representation of methods applicability for explanation of experimental data is according to R^2 value and lower value concerns to error analysis. Although, Langmuir and even Freundlich model have reasonable and acceptable R^2 value, but the applicability of other models such as Tempkin isotherm has commonly been applied in the following linear form [25]: The Tempkin isotherm Eq. (4) can be simplified to the following equation:

$$q_e = \beta \ln \alpha + \beta \ln C_e \quad (3)$$

where $\beta = (RT)/b$ is related to the heat of adsorption, T is the absolute temperature in Kelvin and R is the universal gas constant, $8.314 \text{ (J mol}^{-1} \text{ K}^{-1})$. The adsorption data were analyzed according to the linear form of the Tempkin isotherm.

Kinetic study

The rate as well as mechanism of adsorption process can be elucidated on the basis of kinetic study [25]. Dye adsorption on solid surface may be explained by two distinct mechanisms; (i)

An initial rapid binding of dye molecules on the adsorbent surface followed by (ii) relatively slow intra-particle diffusion. The modeling of the kinetics of present removal studies was investigated by evaluation and analysis of the removal rate to various conventional models like the Lagergren pseudo-first-order model (Eq. (4)) [26], Ho's pseudo second-order model (Eq. (5)):

$$q = q_e (1 - e^{-k_1 t}) \quad (4)$$

$$q = q_e^2 k_2 t / (1 + q_e k_2 t) \quad (5)$$

Where q_e is the amount of AY 199 adsorbed at equilibrium (mgg^{-1}), q is the amount of AY 199 adsorbed at time t (mgg^{-1}), k_1 is the rate constant of pseudo-first-order adsorption (min^{-1}), k_2 is the rate constant of pseudo-second-order adsorption ($\text{gmg}^{-1} \text{ min}^{-1}$). The experimental kinetic results were modeled to above mentioned situations and their estimated parameters values are shown in Table 3. Despite of reasonable value of the R^2 correspond to pseudo-first-order model at 0.03g adsorbent ($R^2 > 0.9521$). Estimated q_e values of pseudo-second-order model accurately predict the adsorption kinetics over the entire working times. Therefore, this model has enough sufficiency for acceptable accurate prediction of the kinetics of AY 199 adsorption onto Ag-NP-AC. The correlation coefficient (R^2) for the pseudo second-order kinetic was above 0.997 and the calculated q_e value has good agreement to the experimental value (Table 3). If the adsorption experiment is a batch system with rapid stirring, there is a possibility that the transport of sorbate from solution into pores (bulk) of the adsorbent is the rate-controlling step. This possibility was tested in terms of a graphical relationship between the amount of dye adsorbed and the square root of

time. The possibility of intra-particle diffusion resistance affecting adsorption was explored by using the intra-particle diffusion model as:

$$q_t = k_{id}t^{1/2} + C \quad (6)$$

In this equation K_{dif} ($mg\ g^{-1}min^{-1/2}$) is the intra-particle diffusion rate constant. The value of K_{dif} was calculated from the slopes of q_t versus $t^{1/2}$. C is the intercept which is related to the thickness of the boundary layer i.e., the larger intercept the greater is the boundary layer effect and their obtained value is reported in Table. 3. The deviation of straight lines from the origin may be because of the difference between the rate of mass transfer in the initial and final stages of adsorption.

It was reported that if the intra particle diffusion is the sole rate-limiting step, it is essential for the q_t versus $t^{1/2}$ plots to pass through the origin that means if the value of C was equal to zero, indicating that the intra particle diffusion model may be the controlling factor in determining the kinetics of the process. The high value of R^2 shows suitability of this model to explain the experimental data. This may confirm that the rate-limiting step is the intra particle diffusion process. Generally, in kinetic studies passing the inter particle diffusion plot through origin show that this mechanism solely limits the adsorption rate [27, 28].

Table 3 Kinetic parameters of AY 199 adsorption onto Ag-NP-AC Conditions: 0.03 g adsorbent over 15 mg L⁻¹ at optima conditions of other variables

Models	parameters	Parameter values: Concentration dye (ppm)	
First order kinetic model: Log (q _e -q _t)=log(q _e)-(K ₁ /2.303)t	K ₁		0.18
	q _e (cal)		9.13
	R ²		0.9521
Second order kinetic model: t/q _t =1/k ₂ q _e ² + (1/q _e)t	K ₂ ×10 ²		33
	q _e (cal)		13.106
	R ²		0.9977
	H		54.24
Intraparticle diffusion q _t =K _{id} t ^{1/2} +C	K _{id}		1.23
	c		5.8
	R ²		0.886
q _e experimental			12.20

Thermodynamic study

Thermodynamic parameters were evaluated to confirm the adsorption nature of the present study.

The thermodynamic constants, free energy, enthalpy and entropy changes were calculated to evaluate the thermodynamic feasibility and the spontaneous nature of the process [29]. The variation of dye removal efficiency with respect to temperature can be explained by thermodynamic parameters, which were evaluated from following Eq.:

$$\Delta G = -RT \ln K, \quad (7)$$

Where ΔG is the free energy change (kJ mol^{-1}), R is the universal gas constant ($8.314 \text{ J mol}^{-1} \text{ K}^{-1}$), K is the thermodynamic equilibrium constant and T is the absolute temperature (K). Values of K may be calculated from the relation $\ln q_e/C_e$ vs. q at different temperatures and extrapolating to zero. The thermodynamic parameters are listed in Table 4. The negative ΔG values confirm the spontaneous nature and feasibility of the adsorption process. The ΔG values were decreased

as the temperature was increased from 283.15–333.15 K, which is an indication of the physical adsorption nature of the process. The values of other parameters such as enthalpy change (ΔH), and entropy change (ΔS), may be determined from Van't Hoff Eq.:

$$\ln K = \Delta S/R - \Delta H/RT. \quad (8)$$

ΔH and ΔG can be obtained from the slope and intercept of Van't Hoff plot of $\ln K$ vs. $1/T$. The data are presented in Table 4. The positive value of ΔH suggested the endothermic nature of adsorption while the positive value of ΔS indicated that the increasing randomness at the solid/solution interface during the adsorption of AY 199 onto Ag-NP-AC. This is the normal consequence of the physical adsorption phenomenon, which takes place through electrostatic interactions.

Table 4 Thermodynamic parameters for adsorption of AY 199 onto 0.03 g of Ag-NP-AC in 50 ml at pH 3 and initial dye concentration of 15 mg L^{-1}

Adsorbent	Parameter	Temperature (K)					
		283.15	293.15	303.15	313.15	323.15	333.15
Ag-NP-AC	value	283.15	293.15	303.15	313.15	323.15	333.15
C_0 (mg L^{-1})	k_c	12	36.01	260.74	1912.67	2600	2704.43
15	ΔG^0 (kJ/mol)	-6	-9.11	-12.23	-20.26	-23.34	-24.12
	ΔS^0 (J/mol K)				383.2		
	ΔH^0 (kJ/mol)				111.23		

CONCLUSION

This investigation shows the efficiency of Ag-NP-AC as a good, green and low-cost adsorbent in compare to the other adsorbents and their doses in removal of dyes. Average adsorption capacity of this adsorbent was 30 mg g⁻¹ for the removal of AY 199 from aqueous solutions in short time (<40 min). In this study, at 25 ±1 °C and the effective pH was 3 and by using 15mgL⁻¹ dye concentration, the adsorbent dose used was found to be 0.03 g/50 mL. Langmuir isotherm gave a better fit to equilibrium data than Freundlich and Tempkin isotherm. The kinetic study of AY 199 on Ag-NP-AC was performed based on pseudo-first order, pseudo-second-order and intra particle diffusion equations. The results of data indicate that the adsorption follows the pseudo-second-order rate in addition to inter particle diffusion model. The present study concludes that the Ag-NP-AC could be employed as low-cost adsorbent instead of commercial activated carbon for the removal of AY 199 from water and wastewater.

REFERENCES

1. Heydari M., Fazaeli R., Yousefi M., 2012. Preparation of Perovskite Nanocomposites and Photochemical Degradation Kinetics of Acid Yellow 199, *J. Appl. Chem Res*, 6:7-15.
2. Wijetunga S., Xiufen L., Wenquan R., Chen J., 2007. Removal Mechanisms of Acid Dyes of Different Chemical Groups under Anaerobic Mixed Culture, *Ruhana J. Scie*, 2: 96-110.
3. Blackburn R. S., 2004. Natural polysaccharides and their interactions with dye molecules: applications in effluent treatment. *Environ. Sci. Technol.* 38: 4905–4909.
4. Crini G., Peindy H. N., Gimbert F., 2007. Removal of C.I. Basic Green 4 (Malachite Green) from aqueous solutions by adsorption using cyclodextrin- based adsorbent: Kinetic and equilibrium studies. *Sep. Pur. Technol*, 53: 97–110.
5. Sun Q., Yang L., 2003. The adsorption of basic dyes from aqueous solution on modeled peat-resin particle. *Water Res.* 37:1535-1544.
6. Yee H., Chin S. M., 2005. Decolorization effects of six azo dyes by O₃, UV/O₃ and UV/H₂O₂ processes. *Dyes Pigm.* 65: 25-31.
7. Chatterjee S., Chatterjee S., Chatterjee B. P., Guha A. K., 2007. Adsorptive removal of congo red, a carcinogenic textile dye by chitosan hydrobeads: Binding mechanism, equilibrium and kinetics. *Colloids & Surfaces A: Physicochem. Eng. Aspects.* 299:146–152.
8. Mondal S., 2008. Methods of dye removal from dye house effluent-an overview. *Environ. Engg. Sci.* 25:383–396.
9. Zonoozi M. H., Moghaddam M. R. A., Arami M., 2009. Coagulation/flocculation of dye containing solutions using polyaluminium chloride and alum. *Water Sci. Technol.* 59:1343–1351.
10. Sachdeva S., Kumar A., 2009. Preparation of nanoporous composite carbon membrane for separation of Rhodamine B dye. *J. Membr. Sci.* 329: 2–10.
11. Tan I., Ahmad A. L., Hameed B. H., 2008. Adsorption of basic dye on high-surface area activated carbon prepared from coconut husk: equilibrium, kinetic and thermodynamic studies. *J. Hazard. Mater.* 154:337–346.
12. Gupta V. K., Jain R., Varshney S., 2007. Electrochemical removal of hazardous dye Reactofix Red 3 BFN from industrial effluents. *J. Colloid Interface Sci.* 312: 292–296.
13. Gupta V. K., 2007. Photochemical degradation of hazardous dye—safaranin-T using TiO₂ catalyst. *J. Colloid Interface Sci.* 309: 460–465.
14. Kavitha D., Namasivayam C., 2007. Experimental and kinetic studies on methylene

blue adsorption by coir pith carbon. *Bioresour. Technol.* 98:14–21.

15. Hua Z., Chena H., Ji F., Yuana S., 2010. Removal of Congo Red from aqueous solution by cattail root. *J. Hazard Mater.* 173:292–297.

16. Cheung W. H., Szeto Y. S., McKay G., 2009. Enhancing the adsorption capacities of acid dyes by chitosan nano particles. *Bioresour. Technol.* 100:1143–1148.

17. Mosallanejad N., Arami A., 2012. Kinetics and isotherm of sunset yellow dye adsorption on cadmium sulfide nanoparticle loaded on activated carbon, *J Chem Health Risks* 2(1): 31-40.

18. Huang H., Yang X., 2004. Synthesis of polysaccharide-stabilized gold and silver nanoparticles: A green method. *Carbohydr. Res.* 339, 2627-2631

19. Huang H., Yang X., 2004. Synthesis of polysaccharide-stabilized gold and silver nanoparticles: a green method. *Carbohydr. Res.* 339: 2627-31.

20. Wang X., Chen Y., 2008. A new two-phase system for the preparation of nearly mono disperse silver nanoparticles, *Mater. Lett.* 62: 4366–8.

21. Goudarzi A., Motedayen Aval G., Park S. S., Choi M.C., Sahraei R., 2009. Antisolvent-induced encapsulation for extraction/preconcentration of silver nanoparticles, *Chem. Mater.* 21: 2375-85.

22. Slejko F. L., 1985. *Adsorption Technology: A Step by step approach to process evaluation application.* Marcel Dekker, NY.

23. Suffet H., McGurie M. J., 1985. Activated carbon adsorption of organics from aqueous phase. *Ann. Arbor. Sci. Michigan.* 1–2.

24. Mittal A., Kurup L., Mittal J., 2007. Freundlich and Langmuir adsorption isotherms and kinetics for the removal of Tartrazine from aqueous solutions using hen feathers. *J. Hazard Mater.* 146:243–248.

25. Langmuir I., 1916. The constitution and fundamental properties of solids and liquids. *J. Am. Chem. Soc.* 38:2221–2295.

26. Crini G., 2006. Non-conventional low-cost adsorbents for dye removal, a review. *Bioresour. Technol.* 97:1061–1085.

27. Temkin M. J., Pyzhev V., 1940. Recent modification to Langmuir isotherms. *Acta Physicochim. USSR.* 12: 217–222.

28. Rengaraj S., Kim Y., Joo C. K., Yi J., 2004. Removal of copper from aqueous solution by aminated and protonated mesoporous aluminas: kinetics and equilibrium. *J. Colloid Interf. Sci.* 273:14-21.

29. Sari A., Tuzen M., 2008. Biosorption of cadmium (II) from aqueous solution by red algae (*Ceramium virgatum*): Equilibrium, kinetic and thermodynamic studies. *J. Hazard. Mater.* 157:448-454.